Bioactive Materials 20 (2023) 434–448

Contents lists available at ScienceDirect

Bioactive Materials

journal homepage: www.keaipublishing.com/en/journals/bioactive-materials

Dual-crosslinked regenerative hydrogel for sutureless long-term repair of corneal defect

Xuanren Shen [a,1], Saiqun Li [b,1], Xuan Zhao [b], Jiandong Han [a], Jiaxin Chen [a], Zilong Rao [a], Kexin Zhang [a], Daping Quan [a], Jin Yuan [b,**], Ying Bai [a,*]

[a] Guangdong Engineering Technology Research Centre for Functional Biomaterials, School of Materials Science and Engineering, Sun Yat-sen University, Guangzhou, 510006, China

[b] State Key Laboratory of Ophthalmology, Zhongshan Ophthalmic Center, Sun Yat-sen University, Guangzhou, 510623, China

ARTICLE INFO

Keywords:
Corneal defect
Decellularized extracellular matrix
Hydrogel
Sutureless repair
Cornea regeneration

ABSTRACT

Corneal transplantation is the most effective clinical treatment for corneal defects, but it requires precise size of donor corneas, surgical sutures, and overcoming other technical challenges. Postoperative patients may suffer graft rejection and complications caused by sutures. Ophthalmic glues that can long-term integrate with the corneal tissue and effectively repair the focal corneal damage are highly desirable. Herein, a hybrid hydrogel consisting of porcine decellularized corneal stroma matrix (pDCSM) and methacrylated hyaluronic acid (HAMA) was developed through a non-competitive dual-crosslinking process. It can be directly filled into corneal defects with various shapes. More importantly, through formation of interpenetrating network and stable amide bonds between the hydrogel and adjacent tissue, the hydrogel manifested excellent adhesion properties to achieve suture-free repair. Meanwhile, the hybrid hydrogel not only preserved bioactive components from pDCSM, but also exhibited cornea-matching transparency, low swelling ratio, slow degradation, and enhanced mechanical properties, which was capable of withstanding superhigh intraocular pressure. The combinatorial hydrogel greatly improved the poor cell adhesion performance of HAMA, supported the viability, proliferation of corneal cells, and preservation of keratocyte phenotype. In a rabbit corneal stromal defect model, the experimental eyes treated with the hybrid hydrogel remained transparent and adhered intimately to the stroma bed with long-term retention, accelerated corneal re-epithelialization and wound healing. Giving the advantages of high bioactivity, low-cost, and good practicality, the dual-crosslinked hybrid hydrogel served effectively for long-term suture-free treatment and tissue regeneration after corneal defect.

1. Introduction

Cornea is a highly transparent tissue located on the outermost part of the eye. It protects the human eye from external intrusion and provides two-thirds of the total refractive power [1]. Corneal injuries and infections are the common causes of corneal scarring and stroma thinning, which can lead to vision loss and even blindness [2]. Transplantation with human donor corneas is currently the most effective clinical treatment of corneal blindness, but healthy implants, advanced surgical skills, and specialized equipment are all required. Nowadays, there is a considerable global donor shortage that limits the corneal transplantation with only one donor cornea available for 70 needed [3]. Meanwhile, the allografts may carry inherent risk of immune rejection and infection, especially in patients with inflammation and severe keratopathy [4,5]. In view of the global shortage of corneal donors, tissue rejection, and stringent surgical requirements, the cost-effective biomaterial-based artificial implants/sealants have become attractive alternatives to promote endogenous regeneration of the cornea [6–8].

Many biomaterials have been investigated for corneal wound healing. For example, pre-formed hydrogels have been extensively studied as corneal substitutes [6,7,9–12], which require precise size and sufficient mechanical strength to withstand surgical sutures [8,13]. Furthermore,

Peer review under responsibility of KeAi Communications Co., Ltd.

* Corresponding author. School of Materials Science and Engineering, Sun Yat-sen University, Guangzhou, 510006, China.

** Corresponding author.

E-mail addresses: yuanjincornea@126.com (J. Yuan), baiy28@mail.sysu.edu.cn (Y. Bai).

[1] Xuanren Shen and Saiqun Li contributed equally.

https://doi.org/10.1016/j.bioactmat.2022.06.006

Received 24 March 2022; Received in revised form 9 June 2022; Accepted 9 June 2022

postoperative complications are often associated with the sutures, including wound leakage, microbial residues, high astigmatism, corneal neovascularization, and graft rejection [14]. In some corneal trauma, the damage occurs within a specific area, where the surrounding tissue remains healthy. Comparing to the transplantation of donor cornea and preformed hydrogels, replacing only the damaged tissue becomes a more attractive strategy for repairing focal corneal defect without extensive replacement and invasive surgery [15]. In-situ-formed transparent hydrogels with tissue adhesion and pre-gel fluidity have become new alternatives in the treatment of corneal injury. The pre-gel solution can flow onto and then gel on the corneal defects to stabilize the corneal wound without suture, promote re-epithelialization and stroma regeneration for vision improvement [16]. Current biomaterials that devoted to corneal sealing and repair include synthetic materials, such as the cyanoacrylate glues, polyethylene glycol (PEG)-based hydrogels, and diverse natural materials (collagen, fibrin, gelatin, alginate, etc.) [17,18]. Cyanoacrylate glue has been used in off-label clinical ophthalmology for years [19,20], but it has obvious disadvantages, including opaque rough surface, rapid polymerization, and high cytotoxicity. Therefore, corneal transplantation is still required [21]. Besides, a few commercial products are only used to close the corneal incisions instead of filling the stroma defects, which limits their clinical use and effect of repair. For example, ReSure Sealant (Ocular Therapeutix) is a PEG-based adhesive that used to close small surgical incisions in cataract surgery. But it has a very short operation window (approximately 30 s), and the effective time is only 1–3 days [22]. Compared to the synthetic materials, natural materials usually possess higher bioactivity. Myung et al. developed an in-situ-formed corneal stromal substitute based on type I collagen and performed a 6-day filling repair on ex *vivo* rabbit corneas [23]. The LC-COMatrix, a modified acellular matrix, was evaluated in animals for a duration of 28 days [24]. Timothy et al. used gelatin-based hydrogels for a four-week repair of focal corneal defects in rabbit eyes [15]. Another gelatin-based hydrogel, GelCORE, was investigated for sutureless corneal defect repair for only two weeks *in vivo* [25]. Ouyang et al. conducted a two-week rabbit study using a molecular coating [26]. These studies have confirmed that the natural biomaterials can promote re-epithelialization of the injured cornea and regeneration of the corneal stroma. However, the long-term effects using hydrogel-based materials have not been fully assessed, at least *in vivo* evaluation that lasted for more than a month has rarely been reported.

Hyaluronic acid (HA) has been widely used in ophthalmology [27–30]. Besides the versatile applications in regenerative medicine, HA often performs as a superb candidate for repairing corneal defects owing to its excellent transparency [17,31–33]. However, previous reports indicated that HA and its derivatives were not conducive to the adhesion of corneal epithelial and stromal cells, which eventually affected the vision recovery [34,35]. Meanwhile, decellularized extracellular matrix (dECM) derived from native tissue/organ has been proven to retain valuable tissue-specificity and high bioactivity for tissue repair [36–39]. Significantly, the decellularized porcine corneas have already been used as tissue-engineered scaffolds for corneal xenotransplantation in clinical practice [40]. Furthermore, dECM hydrogels exhibit low immunogenicity through appropriate decellularization approaches and retain active substances, such as many extracellular matrix structural proteins, glycosaminoglycans, and growth factors [41]. Compared to the single-component natural-material hydrogels, dECM hydrogels better recapitulate the microenvironment of the native tissue, inhibit inflammation [42], provide more cell attachment sites, and promote tissue regeneration [43]. A recent study showed that a decellularized porcine corneal stroma derived hydrogel enabled fast corneal re-epithelialization after gelation at 37 °C [44], but such hydrogel alone exhibited low transparency and weak mechanical strength. The introduction of *N*-cyclohexyl-*N'*-(2-morpholinoethyl) carbodiimide metho-*p*-toluenesulfonate/*N*-hydroxysuccinimide (CMC/NHS) crosslinker significantly improved the strength of decellularized porcine cornea derived hydrogel at room temperature but did not significantly affect its bioactivity [45,46]. However, collagenase and metalloproteinase [47] are secreted abundantly during matrix repair, which may prevent the decellularized cornea hydrogel from long-term retention on corneal defect. Considering that the interpenetration of different macromolecules may lead to a double-network system, the combination of both natural-derived HA and dECM hydrogel is expected to form a mechanically reinforced and more stable bioactive hydrogel for ophthalmological applications.

In this study, we engineered a double-network hydrogel consisting of porcine decellularized corneal stroma matrix hydrogel (pDCSM-G) and methacrylated hyaluronic acid (HAMA) through a non-competitive double crosslinking process using CMC/NHS and phenyl-2,4,6-trimethybenzoylphosphinate (LAP)-induced photocrosslinking, respectively. The pDCSM-G component rendered excellent biological properties to the dual-network hydrogel, and HAMA contributed mainly to the shape and structural stability. After in situ crosslinking, a solid and transparent hydrogel tightly adhered to the stroma bed. Biomolecular compositions, transparency, surface morphology, swelling ratio, and degradation of the hybrid hydrogels were characterized. The mechanical strength and adhesion properties were optimized for tissue-compatible stiffness and adhesiveness. In addition, the cytocompatibility and biological function of the hybrid hydrogel was verified by cell culture. Finally, the operability, adhesive performance, retention, and regeneration of the corneal epithelium and stroma were further evaluated using a rabbit corneal stroma defect model. It was evident that such bioactive dual-crosslinked hydrogel provided promising capabilities of both rapid functional repair of corneal defects without suture and long-term tissue regeneration for complete tissue recovery.

2. Materials and methods

2.1. Materials

HA and CMC were purchased from Macklin (Shanghai, China). NHS was purchased from Aladdin (Shanghai, China). Phosphate-buffered saline (PBS) and all culture related reagents were purchased from Gibco (NY, USA). The genomic DNA kit was purchased from TIANGEN BIOTECH (Beijing, China). The PicoGreen DNA quantification Kit was purchased from ThermoFisher (MA, USA). The glycosaminoglycan (GAG) content kit was purchased from GENMED (Shanghai, China). PrimerScript RT reagent Kit was purchased from TaKaRa Biotechnology (Japan).

2.2. Decellularization

Porcine decellularized corneal stroma (pDCS) was prepared by following a previously reported protocol [39]. Briefly, the porcine corneas were dissected from freshly extracted porcine eyes. After three times of agitation in PBS solution, the corneas were decellularized with 2% Triton X-100 and 1% SDS at 4 °C for 12 h, respectively. Then the resulting pDCSs were rinsed with PBS solution for another three times (30 min each time) prior to lyophilization.

2.3. pDCSM hydrogel preparation

The lyophilized pDCSM was cut into small fragments, then digested in pepsin (10%, w/v) and 0.01 M HCl solution and stirred at room temperature for about 12 h until no visible residual particulates. The pH value of the obtained pDCSM digested solution was gently adjusted to neutral by 5 M NaOH solution, and the ionic balance was adjusted by 10 × PBS solution at 4 °C to obtain 1%, 2%, 3%, and 6% (w/v) pDCSM pregel solutions, respectively.

2.4. HAMA synthesis

HAMA was synthesized by following a reported protocol with slight

modification [48]. 2.0 g HA (400–800 KD) was dissolved in 200 mL deionized water and stirred at room temperature until complete dissolution. 4.0 mL methacrylate anhydride was slowly added to the agitating HA solution at 4 °C. Then the solution was adjusted to pH ~8.0 using 5 M NaOH and reacted for 24 h. During the process, the pH was maintained at 8.0 by constant adjustment using 5 M NaOH. After reaction completed, the product was dialyzed in deionized water for two days with water replacement every 12 h. Finally, the solution was freeze-dried to obtain HAMA powder. The resulting HAMA powder was further dissolved in customized LAP [49,50] solution (0.3% in PBS solution, w/v) to reach concentrations at 1% and 2% (w/v).

2.5. Preparation of pDCSM/HAMA hybrid hydrogels

To obtain the pDCSM/HAMA hybrid hydrogels, different concentrations of the pDSCM pre-gel solutions and 2% (w/v) HAMA pre-gel solutions were mixed at 1:1 vol ratio to reach pDSCM: HAMA (w/w) at ~ 1: 2 (denoted as C1H2) , 1: 1 (C1H1) , 3: 2 (C3H2), and 3: 1 (C3H1), respectively. The hybrid hydrogels were formed by incubated at room temperature for 15–20 min with addition of CMC/NHS crosslinker (molar ratio, n(CMC): n(NHS) = 2: 1), then photocrosslinked with UV light (wavelength ~ 365 nm) for 1 min. As the controls, pDCSM-G were also incubated at room temperature with the same concentration of CMC/NHS crosslinker, 1% HAMA hydrogel were prepared by photocrosslinking using the same light for 1 min. In addition, to demonstrate that CMC/NHS crosslinking helped improving transparency of the pDSCM-containing hydrogels, the pre-gel solutions of C3H1 and 3% (w/v) pDCSM pre-gel solution without CMC/NHS crosslinker were incubated at 37 °C for 15 min to gel.

2.6. Biochemical analysis

DNA, collagen, and GAG contents of the lyophilized pDSCM hydrogel were examined and compared against those of the lyophilized native porcine cornea (NPC). Respectively, the DNA content was extracted using a TIANamp Genomic DNA Kit and quantified by a PicoGreen DNA quantification Kit. The collagen content was determined by measuring the content of hydroxyproline based on p-dimethylaminobenzaldehyde staining. Total collagen content was calculated according to a hydroxyproline: collagen ratio at 1: 7.69 [39,51]. Finally, the GAG content was determined using the glycosaminoglycan content kit by following manufacturer's instructions (n ≥ 3).

2.7. Light transmittance

Disc-shaped hydrogel specimens (1 mm in thickness, 10 mm in diameter) were prepared. The samples were first placed on the papers labeled "SYSU" and imaged to acquire visual representation. Then, the hydrogels were immersed in PBS solution for 1 h to reach equilibrium water uptake state. The light transmittance was measured by ultraviolet–visible spectrophotometer (Lambda 950, PerkinElmer, UK) at wavelength ranging from 380 to 800 nm.

2.8. Scanning electron microscopy (SEM)

The morphology of the hydrogels was characterized by SEM. The hydrogel specimens were pre-lyophilized and placed on the objective tables prior to gold sputtering. The samples were observed, and images were taken using HITACHI S-4800 (Tokyo, Japan) at 10 kV.

2.9. Swelling ratio

The freshly prepared disc-shaped hydrogels (1 mm in thickness, 10 mm in diameter) were weighed (W_0). Then all the hydrogel samples were immersed in PBS solution for 48 h at 37 °C. At different time points, each wet sample were fished out, the residual solution was removed carefully from the surface and the weight was recorded (W_t). The swelling ratio of each sample was calculated by the following equation (Eq. (1)), where W_0 represents the weight of the initial hydrogel, and W_t represents the weight of the sample at different swelling time (n ≥ 5).

$$Swelling\ ratio = \frac{W_t - W_0}{W_0} \times 100\% \quad (1)$$

2.10. Collagenase degradation assay

Disc-shaped hydrogel specimens (1 mm in thickness, 10 mm in diameter) were prepared. The stability of hydrogels was assessed using Type I collagenase (Sigma-Aldrich, Missouri, USA) at 5 U/mL in 0.1 M tris-HCl buffer containing 5 mM $CaCl_2$. The hydrogels were incubated in 37 °C thermostat and weighted after obliterating the surface water at different time points. The percentage of residual mass was calculated by the following equation (Eq. (2)), where W_0' represents the initial weight of the sample, and W_t' represents the sample weight at different degradation time point (n ≥ 5).

$$Residual\ mass\ \% = \frac{W_t'}{W_0'} \times 100\% \quad (2)$$

2.11. Mechanical characterizations

The rheological properties of the hydrogels were evaluated using a Kinexus pro+ rheometer (Malvern Instruments Ltd., UK) with a 20 mm parallel plate. The pre-gel solutions with additional CMC/NHS crosslinker were swiftly placed in the parallel plate with a 0.5 mm gap at 25 °C. The storage modulus (G') and loss modulus(G'') of each hydrogel were recorded in an oscillatory time-sweep mode at 1% strain and a fixed frequency of 1 Hz. To monitor the gelation behaviors of the pDCSM-G and HAMA in the hybrid hydrogel, the sample allowed only the CMC/NHS-based crosslinking for the first 30 min, until exposure to UV light (365 nm, 5 mW/cm^2) for the secondary LAP-initiated photocrosslinking for 5 min (n ≥ 4).

Cylindrical hydrogel specimens (10 mm in thickness, 5 mm in diameter) were prepared for compression test. The samples were pre-immersed in PBS solution for 1h. After fishing out, the diameter and height of each sample were measured by digital caliper. The compression test was implemented using a universal testing machine (CMT5305, SUST, China) at rate = 2 mm/min, maximum strain = 80%. The compressive force and strain were recorded, the compression moduli were calculated by the slope of the linear region on the stress-strain curves (n ≥ 3).

The tensile tests were also carried out using DMA 850 testing machine (TA Instruments, Delaware, USA). Rectangular hydrogel specimens (30 mm in length, 7 mm in width, 1 mm in thickness) were prepared. The two short sides of each sample were gripped by the clamps. The tensile tests were implemented using 2 mm/min rate until rupture. The tensile force and strain were recorded. The tensile strength of each sample was obtained at the breaking point (n ≥ 3).

The shear strength of the hydrogels was determined through lap shear test by following a reported protocol [25]. Two glass slides (76 mm in length, 25 mm in width, 1 mm in thickness) were coated with collagen at 37 °C and air-dried at room temperature. 30 μL pre-gel solution of each hydrogel was evenly applied to the connecting region (25 mm × 10 mm) of the two glass slides and gelled. The lap shear test was implemented using a universal testing machine (CMT5305, SUST, China) at rate of 2 mm/min until the two slides detached. The shear strength was obtained at the point of detachment (n ≥ 5).

2.12. Ex vivo burst pressure test

The adhesive property and sealing ability of the hydrogels were evaluated by a burst pressure test using an artificial anterior chamber.

The pig cornea buttons with sclera were removed from fresh porcine eyes. A corneal perforation was introduced in the center of the button with diameter ~3 mm. The pre-gel solution was injected into the corneal perforation to fill the gap and gelled. The repaired cornea was fixed onto the artificial anterior chamber which was connected to a syringe pump and a pressure gauge detection ranging from 0 to 284.5 mmHg. Pure deionized water was continuously flowed into the artificial anterior chamber driven by a syringe pump, to induce an intraocular-like pressure by a constant increment of 8 mmHg/min until leakage was identified. The bursting pressure of each hydrogel was obtained from the point of leak or fracture ($n \geq 3$).

2.13. In vitro cell studies

2.13.1. Cell culture

Corneal epithelial cells (ATCC CRL-11135) and primary corneal stromal cells were used to characterize the biological performance of the hydrogels *in vitro*. Corneal epithelial cells were cultured in keratinocyte serum free medium (GIBCO-BRL 17005-042) supplemented with 0.05 mg/mL bovine pituitary extract, 5 ng/mL epidermal growth factor, 500 ng/mL hydrocortisone, and 0.005 mg/mL insulin. Primary corneal stromal cells were isolated freshly from New Zealand rabbits and cultured in Dulbecco's modified Eagle medium (DMEM) containing 10% fetal bovine serum (FBS) and 1% penicillin-streptomycin. 3–7 passages of the corneal epithelial cells were used. All cells were cultured in a 37 °C humidified incubator with 5% CO_2, medium was changed every two days.

2.13.2. Cell viability and proliferation

The sterile pre-gel solution was injected into 48-well plates and gelled. The corneal epithelial cells and corneal stromal cells were seeded on the surface of the hydrogels with a density of 4000 cells/well, respectively. The seeded tissue culture plates (TCPs) with the same cell density but without hydrogel coatings were used as control. The viability of the corneal cells was examined using Live/Dead assay kit (KeyGEN BioTECH, Nanjing, China) by following manufacturer's instructions. Live and dead cells were stained with green fluorescence and red fluorescence, respectively, and imaged using an inverted fluorescence microscope (Axio Observer Z1, Carl Zeiss, Germany). The images were analyzed using ImageJ software (NIH, USA). The cell viability on each hydrogel was calculated and represented using the proportion of living cells to the total cells. The experiments sustained for 1, 4, and 7 days, respectively.

The proliferation of the cultured cells was detected by cell counting kit-8 (CCK-8, Dojindo, Japan). The cells were incubated in medium containing 10% CCK-8 for 1 h in the 37 °C humidified incubator with 5% CO_2. Then the absorbance of the stained solution was measured at 450 nm using a microplate reader (Synergy H1, Biotek, VT, USA) after 1, 4, and 7 days, respectively.

2.13.3. Quantitative real-time polymerase chain reaction (qRT-PCR)

The sterile pre-gel solution was injected into 6-well plates and gelled. The corneal stromal cells were seeded on the surface of the hydrogels with a density of 40,000 cells/well. The expression levels of the keratocyte marker keratocan (KERA), corneal proteoglycan lumican (LUM), and the myofibroblast-related genes, collagen1A1 (COL1A1), collagen 3A1 (COL3A1), ACTA2, transforming growth factor beta 1 (TGF-β1) were measured by qRT-PCR. Total RNA was extracted using a RNeasy Plus Mini Kit (TAKARA, Kyoto, Japan) according to the manufacturer's instructions. cDNA was synthesized with PrimerScript RT reagent Kit, and qPCR was performed with PowerUp SYBR Green Master Mix using the CFX 96 touch3 Real-Time PCR system (Bio-rad, USA). Relative gene expression was calculated using the ΔΔCq method after normalization to the reference gene glyceraldehyde-3-phosphate dehydrogenase (GAPDH). The primers sequences were as the following: KERA, forward: 5′-AGTGGAGCTTGGGTCAATCC-3′, reverse: 5′-TGCCATTATACCACCTTGCCT-3′; LUM, forward: 5′-AGATCACGAAGCTCGGTTCC-3′, reverse: 5′-AGGCAGTTTGCTCATCTGGT-3′; COL1A1, forward: 5′-GCAAGAACGGAGATGACGGA-3′, reverse: 5′-TTGGCAC-CATCCAAACCACT-3′; COL3A1, forward: 5′-CCGAACCGTGCCAAATATGC-3′, reverse: 5′-AACAGTGCGGGGAGTAGTTG-3'; ACTA2, forward: 5′- CTCTGGACGTACAACTGGCAT-3′, reverse: 5′- GGAATAGCCACGCTCAGTCA-3′; TGF-β1, forward: 5′-CTCTGGAACGGGCTCAACAT-3′, reverse: 5′-CTCTGTGGAGCTGAAG-CAGT-3′; GAPDH, forward: 5′-ATCCCATCACCATCTTCCAG-3′, reverse: 5′-CCATCACGCCACAGTTTCC-3′.

2.14. Animal studies

2.14.1. Surgical procedures

All animal studies were performed in compliance with the Association for Research in Vision and Ophthalmology (ARVO) Statement for the Use of Animals in Ophthalmology and Vision Research. All experiments were approved by the Animal Care Committees of Zhongshan Ophthalmic Center, Sun Yat-sen University. 8- to 12-week-old male New Zealand white rabbits (supplied by Guangzhou Huadu Hua Dong Xin Hua Experimental Animal Farm, China) were used as animal recipients. The rabbits were anesthetized generally with intravenous injection of 2% pentobarbital sodium (30 mg/kg) and topically with 0.5% proparacaine hydrochloride ophthalmic solution (Alcon Laboratories, FTW, USA). A 3.5 mm trephine was used to create a partial trephination in the center of the cornea with depth = 150–170 μm. The excessive fluid on the recipient stroma bed was wipe-dried with a sponge. CMC/NHS crosslinker was pre-mixed to the pre-gel solution of C3H1 and 3% pDCSM-G. Approximately 10 μL sterilized pre-gel solution was injected onto the prepared corneal defect using a micro-pipette. The pre-gel solution was then carefully adjusted to achieve the suitable curvature and gelled. 15 min after the pre-gel solutions had been applied, HAMA and C3H1 filled eyes were respectively exposed to UV light for 1 min and formed hydrogels in situ, while the CMC/NHS containing pDCSM-G gelled spontaneously within 15–20 min. Then the overflow gel from the defect was cleaned with a sponge. Those rabbits only received corneal defect surgery were used as control group. The experimental eyes were assessed using slit lamp (Topcon system) and anterior segment optical coherence tomography (AS-OCT, Heidelberg Engineering) immediately after surgery. Finally, an Elizabeth collar was employed to prevent the rabbit from eye-scratching. During the first week post-surgery, 0.3% tobramycin/0.1% dexamethasone ointment (Alcon Laboratories) was applied in the operated eyes on daily basis.

2.14.2. Slit lamp, AS-OCT, and confocal microscopy observations

The slit lamp was used weekly to observe the transparency, curvature integrity, inflammatory reaction, and other abnormalities of the experimental eyes. Fluorescein staining was applied to evaluate the epithelial defect area. Cross-sectional photographs of cornea were taken weekly using AS-OCT to further evaluate curvature, hydrogel degradation, and adhesive performance of the hydrogels on the stroma bed. Confocal microscopy (IVCM, Confoscan 4, Nidek, Japan) was employed to evaluate the deeper optical nerve, stromal layer, and endothelial layer at the injury site after eight weeks.

2.14.3. Histological analysis

The animals were euthanized after 8 weeks. The corneas were harvested and fixed with 4% paraformaldehyde. Frozen sections were obtained after embedding in optimal cutting temperature compound. The cryo-sections were subjected to hematoxylin and eosin (H&E), Masson trichrome staining and immunofluorescence staining. A mouse monoclonal anti-α-SMA IgG primary antibody (1:5000, Abcam) and an HRP-conjugated rabbit anti-mouse IgM secondary antibody (1:1000, Bioss) were used for immunostaining assays. Images were captured using an inverted fluorescence microscope (Axio Observer Z1, Carl Zeiss, Germany) and a laser scanning confocal microscope (LSM 710 NLO, Carl Zeiss, Germany), respectively.

2.15. Statistical analysis

The data were conveyed as means ± standard deviation. Student's t-test were performed to compare mean value between groups using GraphPad Prism 9 (GraphPad Software, USA). A value of $P < 0.05$ was considered statistically significant difference.

3. Results

3.1. Preparation of the dual-crosslinked hydrogels

HA were pre-functionalized with methacrylic anhydride, so that the resulting HAMA can undergo photocrosslinking with presence of the photoinitiator LAP (Fig. S1A). Meanwhile, the pDCSM-G alone can be chemically crosslinked by CMC/NHS (Fig. S1B). To obtain a more robust hybrid hydrogel system through formation of interpenetrating network, the HAMA and pDCSM pre-gel solutions were pre-mixed with additional LAP and CMC/NHS, both crosslinking modes were induced simultaneously to reach a dual-crosslinked hybrid hydrogel with excellent intermolecular compatibility. For treatment of corneal defects, the pre-mixed HAMA/pDCSM solution was first injected into the defected region. Amide bonds formed within the hydrogel and between the hydrogel and adjacent tissue with the presence of CMC/NHS, then the hybrid hydrogel spontaneously formed in situ after a short-term UV exposure, typically no more than 1 min (Fig. 1A).

In addition to the preparation of the hydrogels, the extent of decellularization was assessed regarding the residual DNA, collagen, and GAG contents detected in the pDCSM-G, and compared to those in the native cornea tissue (i.e., the NPC). Quantitative analysis showed that the lyophilized pDCSM-G contained 19 ± 3 ng/mg of the total DNA content, which was only ~10% of that found in the NPCs (186 ± 18 ng/mg, Fig. 1B), indicating a rather complete removal of genetic antigens. On the other aspect, no significant reduction in collagen and GAG contents was evident between pDCSM-G and NPC (Fig. 1C and D), which

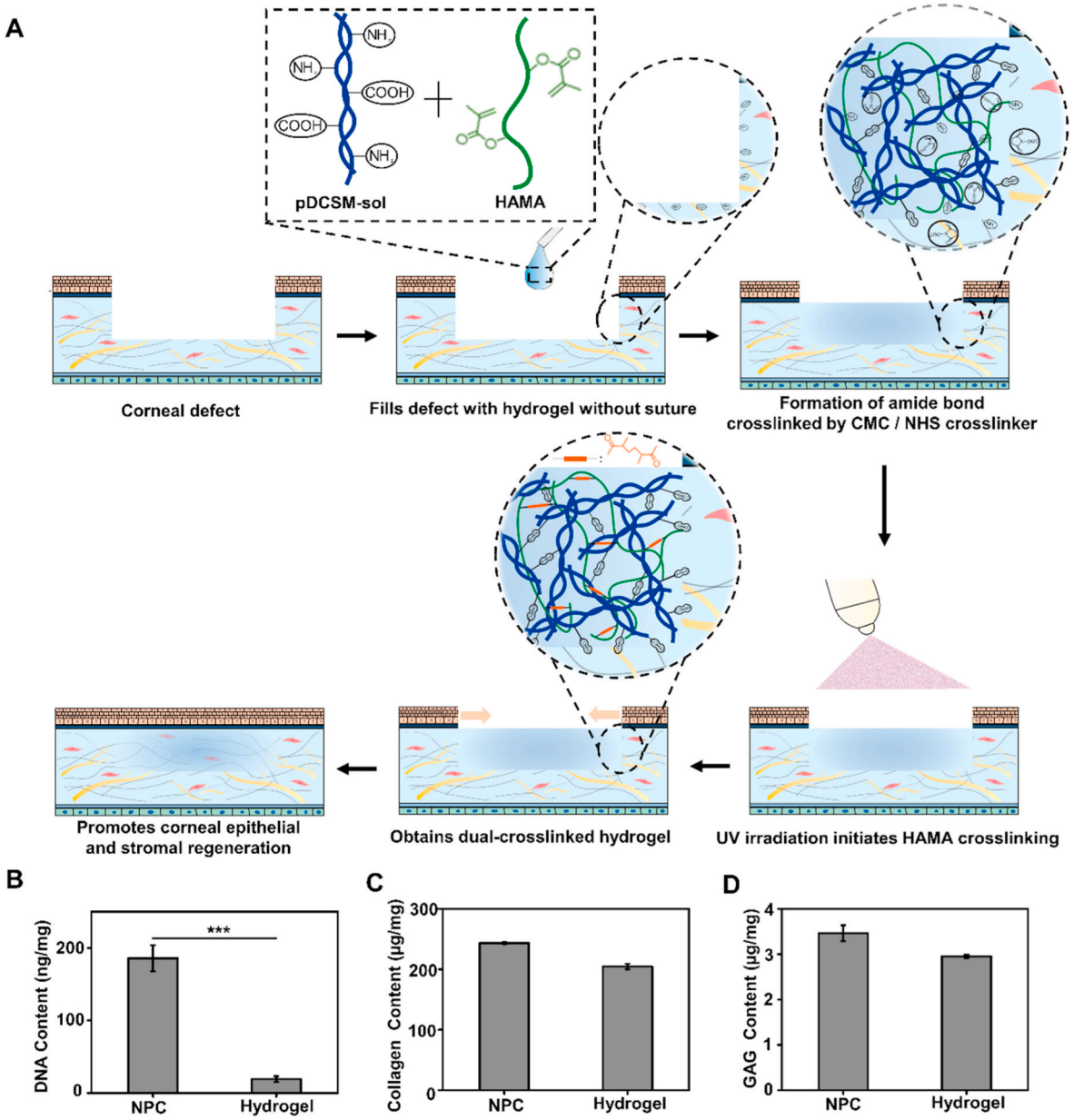

Fig. 1. Application, synthesis, and biomolecular compositions of hydrogels. (A) Schematic illustrations of the hybrid hydrogel applied onto corneal defect in situ for long-term regenerative repair. Quantitative analysis of the (B) DNA, (C) collagen, and (D) GAG contents in the NPCs and those retained in the pDCSM-G, respectively. (***, $P < 0.001$).

implicated a considerable preservation of the structural and functional compositions to retain the biological properties after decellularization.

3.2. Chemical crosslinking endows hydrogels with high transparency and slow degradation

It was obvious that the chemically crosslinked hydrogels, including the photocrosslinked HAMA (1%, w/v), CMC/NHS crosslinked pDCSM-G (3%, w/v), and the dual-crosslinked hybrid hydrogel, exhibited excellent transparency (Fig. 2A). The light transmittance of these hydrogels was all above 80% within wavelength range of visible light (380–800 nm, Fig. 2B). It was also noted that the pDCSM pre-gel solution without CMC/NHS gelled spontaneously at ~37 °C via β-sheet formation [38], hydrogel bonding, and other physical crosslinking mechanisms. However, the physically crosslinked pDCSM-G was relatively opaque, even with the combinatorial photocrosslinked HAMA component (Fig. 2A and B). Since maintaining high corneal transparency is critical in ophthalmic treatments, the pDCSM-containing hydrogels are required to be chemically crosslinked.

The swelling ratio and enzymatic degradation are key indicators to evaluate the shape and structural stability of the hydrogels. Swelling characterization showed that the CMC/NHS crosslinked 3% pDCSM-G exhibited the largest swelling ratio (6.85 ± 0.30%) among all prepared hydrogel specimens after two days of immersion in PBS solution (Fig. 2C). The photocrosslinked 1% HAMA underwent the second largest swelling ratio (5.86 ± 0.44%). Once the CMC/NHS containing pDCSM-G was integrated into HAMA, the swelling effect of the hybrid hydrogels became significantly alleviated following dual-crosslinking. In the hybrid hydrogel samples, the composition of HAMA component was maintained at 1% (w/v), and the concentration of the pDCSM-G was varied at 0.5% (C1H2), 1% (C1H1), 1.5% (C3H2), and 3% (C3H1). It was noted that the swelling ratio decreased with increasing the pDCSM component within the hydrogels (Fig. S2), which was attributed to the higher crosslinking density. In our experiment, the smallest swelling ratio was reached by the dual-crosslinked C3H1 hydrogel. Similar trend was evident in the degradation assessments with the presence of collagenase type I. The C3H1 hydrogel retained more than 70% of the original mass (Fig. 2D) and the initial disc shape after 8 weeks of degradation (Fig. S3). In contrast, the CMC/NHS crosslinked pDCSM-G degraded much faster than the hybrid hydrogels and 1% HAMA (Fig. S4). The integration of HAMA network significantly improved both compositional and structural stability of the hybrid hydrogel, implicating that the dual-crosslinked hydrogel can provide long-term retention in corneal defects.

In addition, the ultrastructure of the hydrogels was assessed by SEM, which showed that all the HAMA, pDCSM-G, and the hybrid hydrogels exhibited micro-porous 3D network structures which enable cell adhesion and penetration [52]. Among them, the hybrid C3H1 hydrogel had the densest porous structure with pore sizes ranging from 50 to 150 μm (Fig. 2E), due to the macromolecular entanglement of both gel networks. The results from Fourier transform infrared spectroscopy by comparison between C3H1 hydrogels before and after dual-crosslinking indicated a successful preparation of the hybrid hydrogel (Fig. S5).

3.3. Dual-crosslinked hydrogels possess enhanced mechanical properties

The mechanical properties of the hydrogels were examined by rheology, compression, and tensile tests. First, to better understand the rheological performance of the hydrogels before and after photocrosslinking, the 1% HAMA, 3% pDSCM-G with CMC/NHS, and the C3H1 hybrid hydrogels were only exposed to UV light (wavelength ~ 365 nm) only at the pre-determined time point of the rheology measurement. It was evident that the HAMA was in a flow dynamic state (storage modulus $G' <$ loss modulus G'') before light exposure, then the storage modulus elevated to a plateau immediately after the light turned on, suggesting a quick photocrosslinking to form HAMA hydrogel (Fig. S6A). For the CMC/NHS containing pDCSM-G, G' was always higher than G'', and both G' and G'' gradually increased over time, indicating a relatively slow chemical crosslinking process (Fig. S6B). The rheological characterization of the C3H1 hybrid hydrogel conveyed both performance, which gradually gelled at the beginning, once exposed to irradiation, it rapidly formed into a more robust hydrogel with double-network structure (Fig. 3A). The final storage modulus of the C3H1 hydrogel ($G' = 4326 \pm 73$ Pa) was greater than those of the 1% HAMA hydrogel ($G' = 3131 \pm 101$ Pa) and 3% pDCSM-G ($G' = 3073 \pm 195$ Pa, Fig. 3B) after 1 min of light exposure.

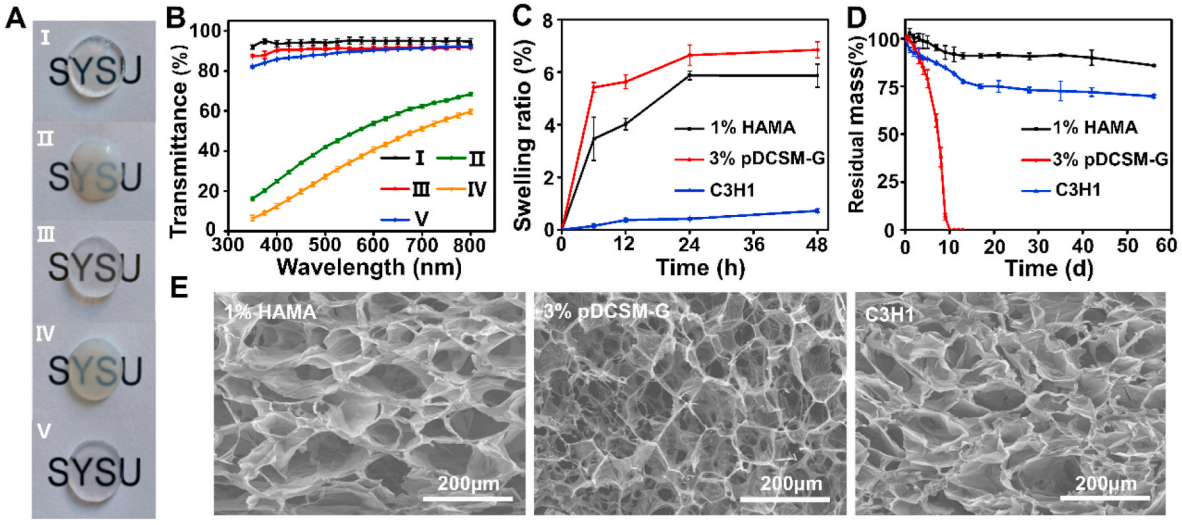

Fig. 2. Optical, swelling, degradation, and microscopic characterizations of the hydrogels. (A) Photographs of the prepared hydrogel specimens (thickness ~ 1 mm) placed on an "SYSU"-labeled paper. The five hydrogel specimens were, (I) photocrosslinked 1% HAMA, (II) physically crosslinked 3% pDCSM-G without CMC/NHS at 37 °C, (III) CMC/NHS crosslinked 3% pDCSM-G, (IV) photocrosslinked C3H1 hybrid hydrogel without CMC/NHS at 37 °C, and (V) dual-crosslinked C3H1 hydrogel. (B) Light transmittance of the abovementioned five hydrogel specimens on visible light spectrum. (C) Swelling ratios of the photocrosslinked 1% HAMA, CMC/NHS crosslinked 3% pDCSM-G, and dual-crosslinked C3H1 hydrogels when immersed in PBS solution at 37 °C in PBS solution within two days, respectively. (D) Long-term degradation behavior of the photocrosslinked 1% HAMA, CMC/NHS crosslinked 3% pDCSM-G, and dual-crosslinked C3H1 hydrogels in 5U/mL collagenase type I solution at 37 °C within 60 days, respectively. (E) SEM micrographs of the lyophilized photocrosslinked 1% HAMA, CMC/NHS crosslinked 3% pDCSM-G, and dual-crosslinked C3H1 hydrogels.

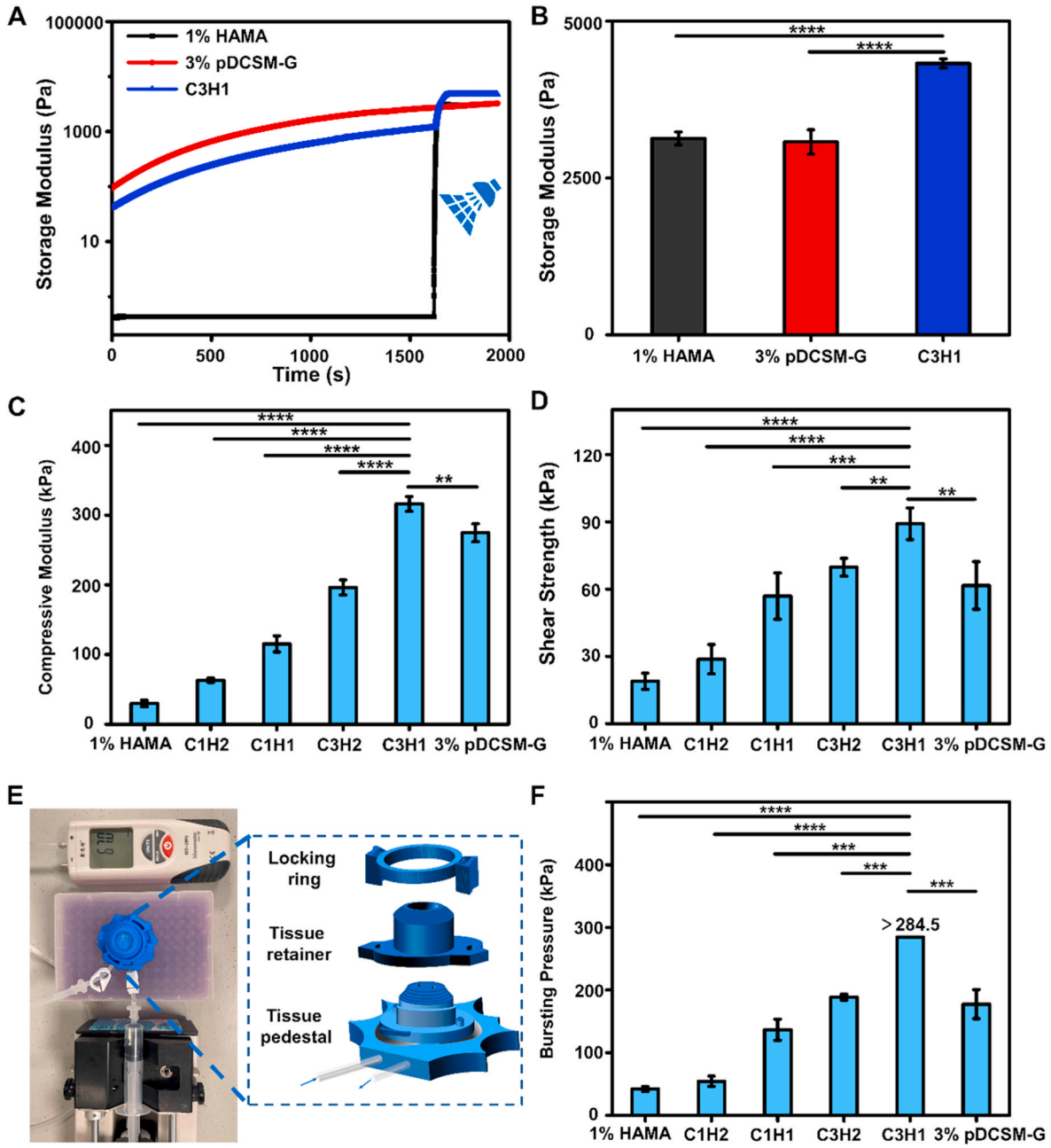

Fig. 3. Mechanical characterizations of the chemically crosslinked hydrogels. (A) Rheological characterization of the photocrosslinked 1% HAMA, CMC/NHS crosslinked 3% pDCSM-G, and dual-crosslinked C3H1 hydrogel before and after light exposure. (B) storage moduli of the 1% HAMA, 3% pDCSM-G, and C3H1 hydrogels after chemical crosslinking, characterized by rheometry. (C) Compressive moduli of the hydrogels with different compositions of HAMA and pDCSM-G. (D) Shear strength of the hydrogels with different compositions of HAMA and pDCSM-G. (E) Photograph of the artificial anterior chamber device used for bursting pressure tests. (F) Averaged bursting pressures of the hydrogels with different compositions of HAMA and pDCSM-G. (**P < 0.01, ***P < 0.001, ****P < 0.0001).

Next, the mechanical properties, including the compressive moduli and shear strength, of the dual-crosslinked hybrid hydrogel specimens were evaluated, in comparison with the photocrosslinked 1% HAMA and CMC/NHS crosslinked 3% pDCSM-G. It was noted that the compressive moduli increased with constant increment of the pDCSM concentration in the hybrid hydrogels, i.e., from 1% HAMA to C3H1 hydrogel, the compressive moduli were significantly elevated from 30 to 316 kPa (Fig. 3C), which comprise that of the native cornea (115 ± 13 kPa) [25]. Among these hybrid hydrogels, C3H1 not only possessed the highest compressive modulus, but also exhibited superior deformation resistance property due to the tensile strength ~43 kPa (Fig. S7). While the other hydrogels, including 1% HAMA, C1H2, C1H1, C3H2, and 3% pDCSM-G were easily cracked by the clamps of the testing machine. The increase in hydrogel strength was attributed to the higher crosslink density in the hydrogel network. A denser crosslinking network made the hydrogel more resistant to external impacts.

Finally, the hydrogel used for sutureless repair of corneal injuries requires sufficient adhesion with adjacent tissues that withstands high intraocular pressure (IOP) and avoid detachment from the eye. To this end, we further characterized the adhesion properties of the hydrogels, including shear strength and burst pressure. To investigate the shear strength, a layer of gelatin was pre-coated on the surface of a glass slide to mimic the tissue environment, and the pre-gel solutions were evenly applied to the designated area, then subjected to tensile testing following chemical crosslinking. The results showed that the shear strength of the chemically crosslinked hydrogels followed the similar

trend as the compressive moduli (Fig. 3D). Especially, the maximum shear strength (89 ± 7 kPa) was reached by C3H1 hydrogel, which is even more than the sum of those of individually crosslinked 1% HAMA (19 ± 4 kPa) and 3% pDSCM-G (62 ± 11 kPa). The adhesive property of the hydrogels was further verified ex vivo using an artificial anterior chamber (Fig. 3E). We manually introduced a corneal perforation (diameter ~ 3 mm) on each freshly dissected porcine cornea, filled with a pre-gel solution, then chemically crosslinked in situ. Deinoized water was slowly injected into the chamber to induce IOP-like inner pressure. The inner pressure was recorded as the burst pressure when leak/spurt was identified at the defected region (Fig. 3F). It was evident that the burst pressures of all hydrogel-filled specimens were significantly higher than the normal intraocular pressure in the eye (10–21 mmHg). The dual-crosslinked C3H1 hydrogel withheld the largest burst pressure, which even exceeded the full measuring range of the pressure gauge (>284.5 mmHg).

In general, the dual-crosslinked C3H1 hydrogel exhibited the greatest force-resistance and corneal adhesion capability, minimized swelling ratio, and slow degradation during enzymatic hydrolysis among all chemically crosslinked hydrogels with different compositional variations. Therefore, C3H1 hydrogel was chosen for the following *in vitro* cell studies and in *vivo* assessments for corneal defect repair and tissue regeneration.

3.4. Dual-crosslinked hydrogel exhibits excellent cytocompatibility and biological properties for corneal cells

To verify the cytocompatibility of the dual-crosslinked C3H1 hydrogel, human corneal epithelial cells and primary rabbit corneal stromal cells were respectively used for *in vitro* cell culture on the hydrogels, while 1% HAMA, 3% pDCSM-G, and tissue culture plates (TCP) were employed as the control groups.

First, corneal epithelial cells were pre-seeded and cultured on the hydrogels and TCP, then their viability and proliferation were evaluated by Live/Dead and CCK-8 assays on Day 1, 4, and 7. It was noted that very few epithelial cells were identified on the HAMA hydrogels even after 7 days of culture (Fig. 4A, Fig. S8). Since the epithelial cells hardly attached to the HAMA hydrogel, their viability was much lower than those cultured on other hydrogels (Fig. 4B). Meanwhile, the epithelial cells accommodated well on the pDCSM-G containing hydrogels (pDCSM-G and C3H1), they not only exhibited high viability (>95%) comparable to those cultured on TCP (Fig. 4B) but also facilitated cell spreading and proliferation. Results from CCK-8 assay showed that the OD values significant increased with prolonging the incubation time on both C3H1 hydrogel and pDCSM-G, compared to those cultured on the HAMA hydrogel (Fig. 4C), indicating a good proliferation rate. Similarly, the C3H1 hydrogel supported the adhesion of primary corneal stromal cells compared to HAMA hydrogel (Fig. 4D, Fig. S9). The viability of live stromal cells on C3H1 hydrogel were close to other cultured on pDCSM-G and TCP (Fig. 4E). The CCK-8 assay further showed that C3H1 hydrogel facilitated the stromal cells proliferation (Fig. 4F).

Furthermore, we analyzed the expression of keratocyte marker keratocan [53], critical corneal proteoglycan lumican, myofibroblast-related genes COL1A1, COL3A1, ACTA2, and TGF-β1 to verify the cell-matrix interaction of C3H1 hydrogel on the corneal stromal cell phenotypes. qRT-PCR results showed that much higher expression of keratocan and lumican, but relatively lower expression of myofibroblast-related genes COL1A1, COL3A1, ACTA2, and TGF-β1 of corneal stromal cells was evident on the C3H1 hydrogel, compared with those cultured on TCPs (Fig. 4G).

The results from *in vitro* cell culture revealed the high bioactivity of the pDCSM components in dual-crosslinked C3H1 hydrogel, which endowed the hybrid hydrogel with excellent biocompatibility, facilitated cell adhesion, viability, and proliferation, as well as contributed to maintain the keratocyte phenotype.

3.5. Dual-crosslinked hydrogel performs fast re-epithelialization and long-term retention for corneal defect repair in vivo

To evaluate the feasibility of the chemically crosslinked hydrogels for potential clinical applications, rabbit corneal defect model was established by using trephination to introduce a cylindrical defect in the stroma with ~3.5 mm in diameter. The pre-gel solution was directly perfused onto the defected region of the corneal stroma, after the gap was fully filled, the curvature of the pre-gel solution can be carefully adjusted using a scraper within ~10 min. 15 min after the pre-gel solutions had been applied, HAMA and C3H1 filled eyes were respectively exposed to UV light for 1 min and formed hydrogels in situ, while the CMC/NHS containing pDCSM-G gelled spontaneously within 15–20 min (Fig. 5A). Slit lamp photographs and cross-sectional AS-OCT images of the hydrogel-treated corneas showed that the corneal defects were completely filled by C3H1 hydrogel (Fig. 5B), HAMA hydrogel (Fig. 5C), and pDCSM-G (Fig. 5D), respectively, which adhered well to the stromal beds. All the applied hydrogels exhibited smooth surfaces with no obvious adverse reactions in the rabbit eyes post-surgery. AS-OCT characterization showed that the C3H1 and pDCSM-G exhibited similar optical reflectivity as the surrounding corneal stroma, in contrast to HAMA hydrogel. Such observations suggested greater resemblance of the pDCSM-containing hydrogels to the native corneal tissue [24].

After the hydrogel treatments on rabbit corneal defects, we characterized the re-epithelialization by fluorescein staining, and compared between the defected eyes treated by C3H1 and HAMA hydrogels (Fig. 6A). It was clearly observed that the epithelial defect area progressively decreased in the C3H1 hydrogel filled eyes, the re-epithelialization was completed during the third week, implicating constant epithelial migration on the hydrogel. While the pDCSM-G treated eyes exhibited even faster re-epithelialization, in which group, the epithelial defect almost disappeared after two weeks (Fig. S10). In contrast, no obvious shrinkage of epithelial defect area was evident on the HAMA hydrogel treated eyes during the first three weeks. Even after six weeks postoperatively, there were still some minor epithelial defects (Fig. 6A).

An eight-week-long observation on the experimental eyes was implemented in this study, no obvious inflammatory reaction or neovascularization was observed during the long-term hydrogel retention. Four weeks after surgery, the C3H1 hydrogel treated corneas showed good transparency and smooth surface, while obvious corneal scar formation (significant interface haze observed on the AS-OCT photographs) was evident in the corneal defects filled with HAMA hydrogel, possibly due to the failure of re-epithelialization. The slit lamp and AS-OCT photographs indicated that the cornea filled with C3H1 hydrogel maintained a desirable curvature after the first month, considerable volume of the dual-crosslinked hydrogel was intimately adhered to the stroma bed (Fig. 6B). In comparison to the C3H1 hydrogel, the HAMA hydrogel was delaminated at the surgical section and the originally defected region became opaque (whitish color). Meanwhile the in situ filled pDCSM-G completely degraded, evident by the discontinuous slit lamp light on the experimental eye and obvious pit on the AS-OCT image, despite that the pDCSM-G treated cornea remained transparent. After two months postoperatively, the C3H1 hydrogel treated corneas still exhibited good transparency and appropriate curvature. While obvious delamination-like surface was still observed on the pDCSM-G filled eyes even after complete re-epithelialization. Moreover, corneal scars shown as the interface haze on the AS-OCT images were easily identified at the defected sites in the eyes treated with HAMA hydrogel and pDCSM-G, but not evident in the C3H1 treated eyes (Fig. 6B). *In vivo* confocal microscopic appearance further confirmed that no obvious scar formation was identified within the C3H1 hydrogel treated corneas. Underlying corneal stromal cells can be easily observed without any patchy hyperreflection, showing no evidence of excessive corneal scarring. Additionally, the nerves in the deeper layers and the endothelial layer were also visible and remained intact eight weeks post-

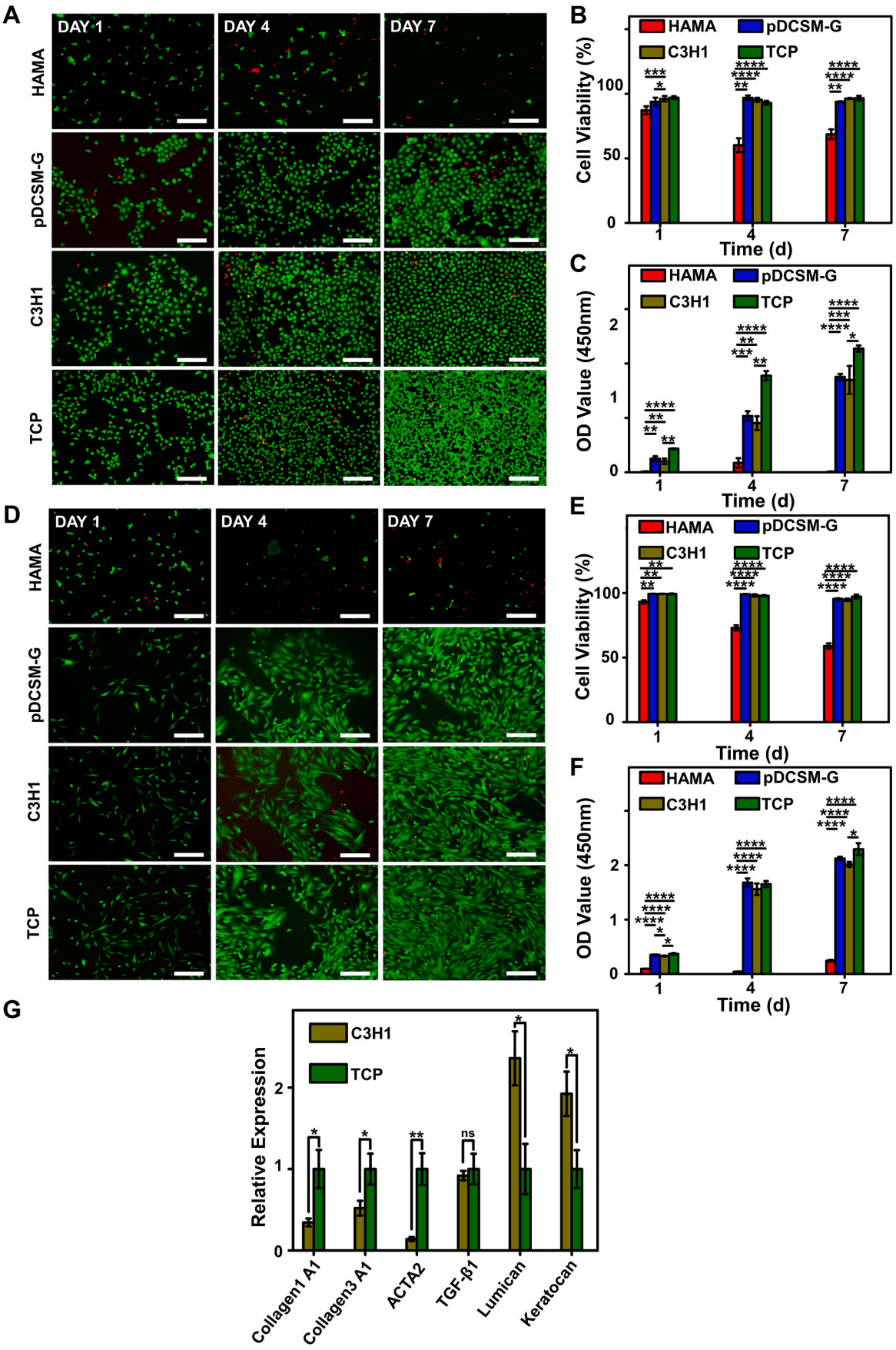

(caption on next page)

Fig. 4. Corneal epithelial cells and corneal stromal cells cultured on the HAMA, pDCSM-G, C3H1 hydrogels, and TCP. (A) Live/Dead staining of corneal epithelial cells cultured on 1% HAMA, 3% pDCSM-G, C3H1 hydrogel, and TCP for 1, 4, and 7 days, respectively. Scale bars = 200 μm. (B) Quantification of the corneal epithelial cells viability on hydrogels and TCP characterized by Live/Dead assay. (C) CCK-8 assay of the cultured corneal epithelial cells after 1, 4, and 7 days. (D) Live/Dead staining of corneal stromal cells cultured on 1% HAMA, 3% pDCSM-G, C3H1 hydrogel, and TCP for 1, 4, and 7 days. Scale bars = 200 μm. (E) Quantification of the corneal stromal cells viability on hydrogels and TCP characterized by Live/Dead assay. (F) CCK-8 assay of the cultured corneal stroma cells after 1, 4, and 7 days. (G) qRT-PCR analysis of the relative mRNA expression levels of Collagen 1A1, Collagen 3A1, ACTA2, TGF-β1, lumican, and keratocan in the rabbit corneal stromal cells after culturing on the C3H1 hydrogel and TCP for four days. (*P < 0.05, **P < 0.01, ***P < 0.001, ****P < 0.0001).

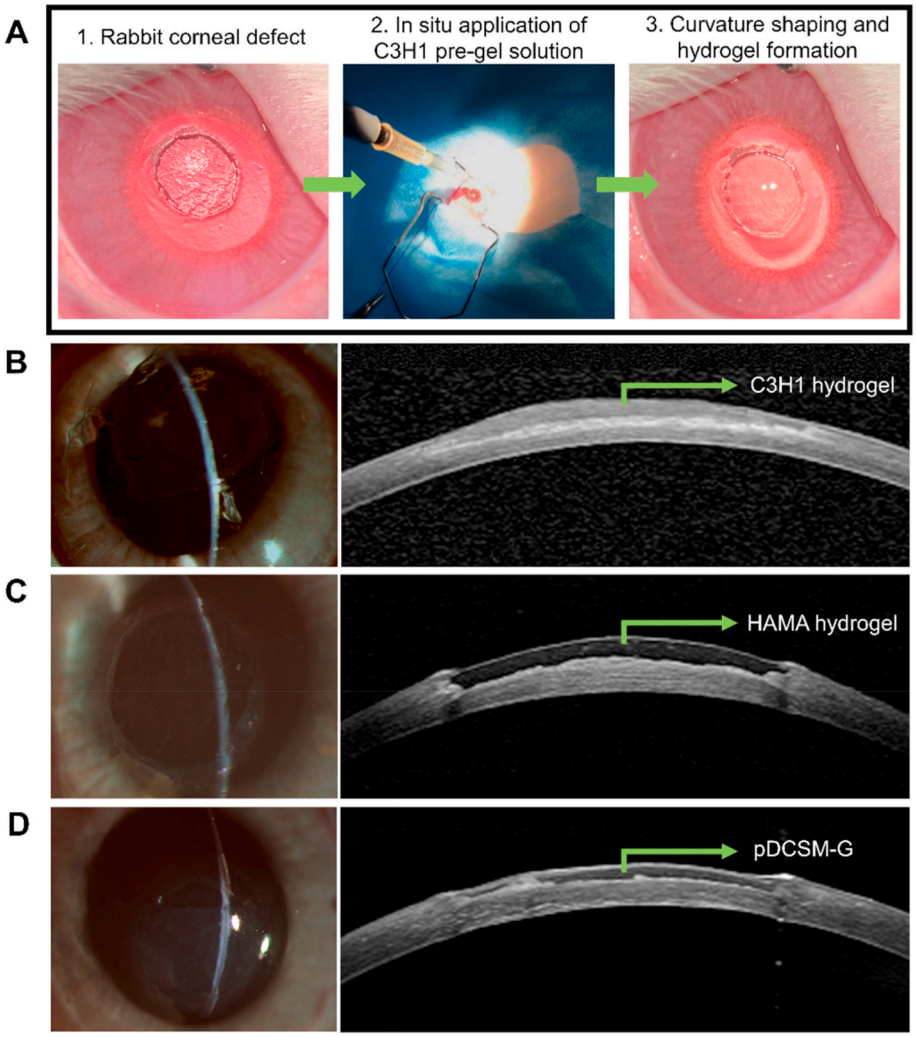

Fig. 5. *In vivo* application of the hydrogels onto rabbit corneal defects. (A) Procedure of hydrogel injection onto the corneal defect. Representative slit lamp photographs (left) and AS-OCT images (right) after hydrogel treatments using (B) C3H1 hydrogel, (C) 1% HAMA hydrogel, and (D) 3% pDCSM-G, respectively.

operation (Fig. 6C), implicating that C3H1 hydrogel did not cause any damage to the posterior stroma.

3.6. Dual-crosslinked hydrogel promotes long-term regeneration of corneal tissue

Histological examinations were performed on the cryo-sectioned corneal tissues eight weeks post-surgery. The extent of epithelium regeneration was first evaluated by H&E staining. It was noted that the defected corneas without hydrogel treatment exhibited significant epithelial hypertrophy (Fig. 7B). On the contrary, the corneas filled with HAMA hydrogel and pDCSM-G only formed single layer of epithelial cells (Fig. 7C and D). The dual-crosslinked C3H1 hydrogel helped construction of a new epithelium with three to four epithelial cell layers (Fig. 7E), which was even comparable to that on a native cornea (Fig. 7A). The statistical results confirmed that the epithelium thickness of the C3H1 treated corneas (37 ± 4 μm) was closest to that of the native corneas (33 ± 1 μm), while both HAMA and pDCSM-G treated ones were much thinner (Fig. 7F).

The histological characterization also revealed that the C3H1 hydrogel filled corneal stroma underwent highly ordered arrangement and regeneration at the defected site. Meanwhile, the HAMA hydrogel and pDCSM-G filled corneas, as well as the untreated ones retained obvious defects with insufficient thickness (Fig. 7ÃE). The corneal stroma thickness of the C3H1 treated eyes (458 ± 19 μm) was the closest to that of the native corneas (490 ± 5 μm), the other groups all resulted in much thinner stroma.

Additionally, to examine inflammation in the experimental eyes, immunofluorescence staining was used for α-SMA associated corneal scars. It was noted that the α-SMA expression in both the HAMA hydrogel (Fig. 7J) and pDCSM-G (Fig. 7K) treated stroma was significantly higher than that of the C3H1 group (Fig. 7L) which was similar to

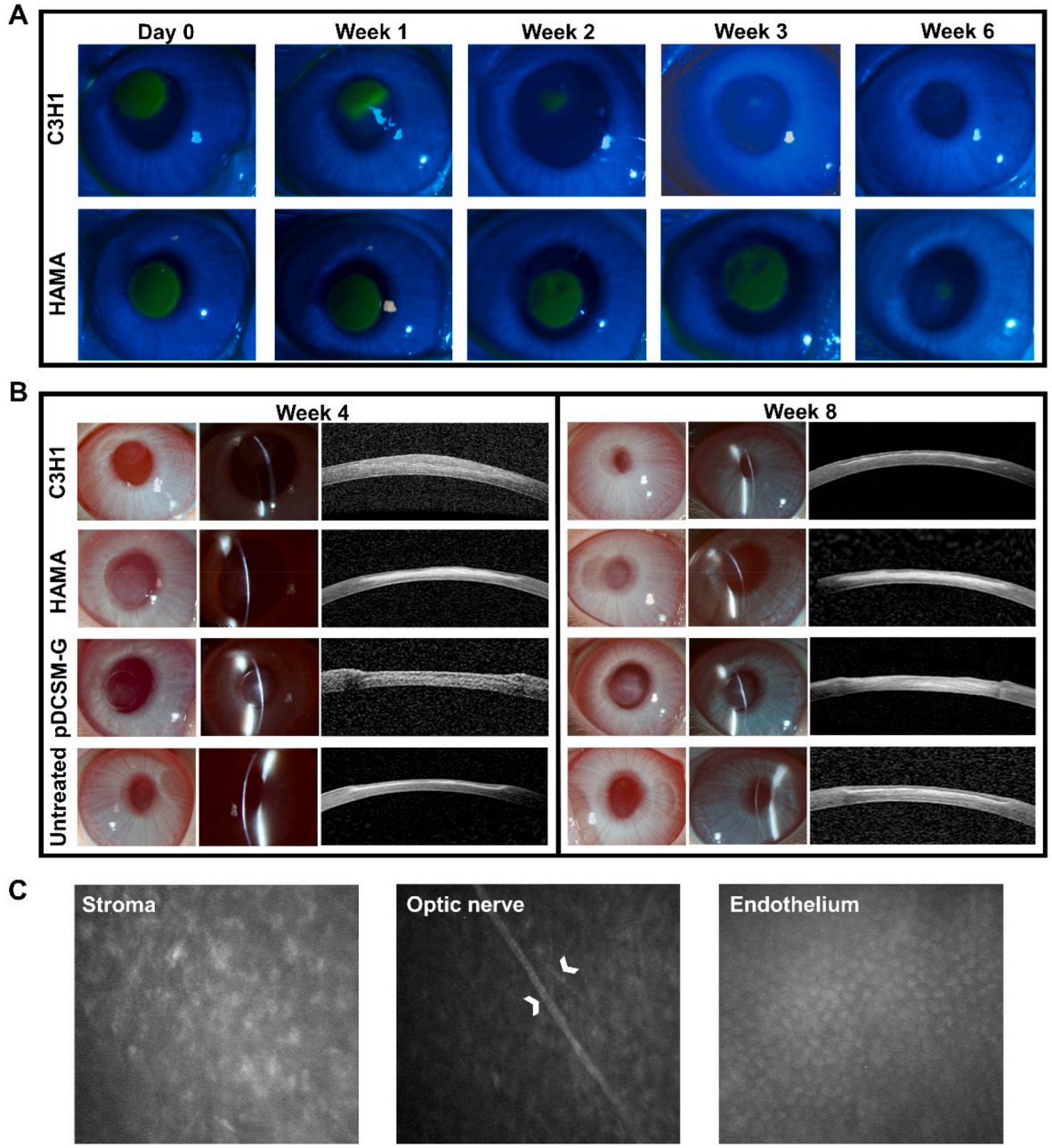

Fig. 6. Postoperative observation of the hydrogel treated corneas. (A) Representative photographs of cobalt blue with fluorescein staining in the rabbit experimental eyes filled with C3H1 and 1% HAMA hydrogels at different time points. The green area in the central cornea indicates the epithelial defect. (B) Representative slit lamp and AS-OCT images of the experimental eyes filled with C3H1 hydrogel, 1% HAMA hydrogel, 3% pDCSM-G, and the untreated eyes 4 and 8 weeks after surgery. (C) Confocal micrographs of the corneal stroma, optic nerve, and endothelium in the C3H1-hydrogel-filled cornea 8 weeks post-operation. White arrows point at the optic nerves of the posterior stroma.

that of the native cornea tissue (Fig. 7H). Such results indicated that significant scar formation led to irreversibly reduced transparency of the HAMA and pDCSM-G treated corneas (Fig. 6B), but minimal inflammation occurred to the dual-crosslinked hydrogel filled eyes for at least two months after surgery. Masson trichrome staining (Fig. S11) further revealed that the C3H1 hydrogel promoted collagen fiber (blue) regeneration compared to the HAMA hydrogel and pDCSM-G. The corneal defects filled with HAMA hydrogel and pDCSM-G were found associated with significant fibrosis (red fibers) in the stroma (pointed out by the yellow arrows in Fig. S11).

4. Discussion

The hydrogel derived from decellularized cornea possesses unique advantages in preserving corneal stromal keratocyte cells, facilitating rapid re-epithelialization, and promoting corneal tissue regeneration, which have brought great interests in potential treatments of corneal diseases, especially for corneal wound healing [24,44,54,55]. However, the dECM hydrogel often suffer from their low mechanical strength and fast degradation, even after chemical crosslinking [56], which is unsatisfied for long-term repair of corneal defects with critical optical functional (i.e., enough transparency) and tissue regeneration requirements. Herein, we aim to develop a dECM-containing hydrogel that qualify long-term retention in the corneal defect, which also provides

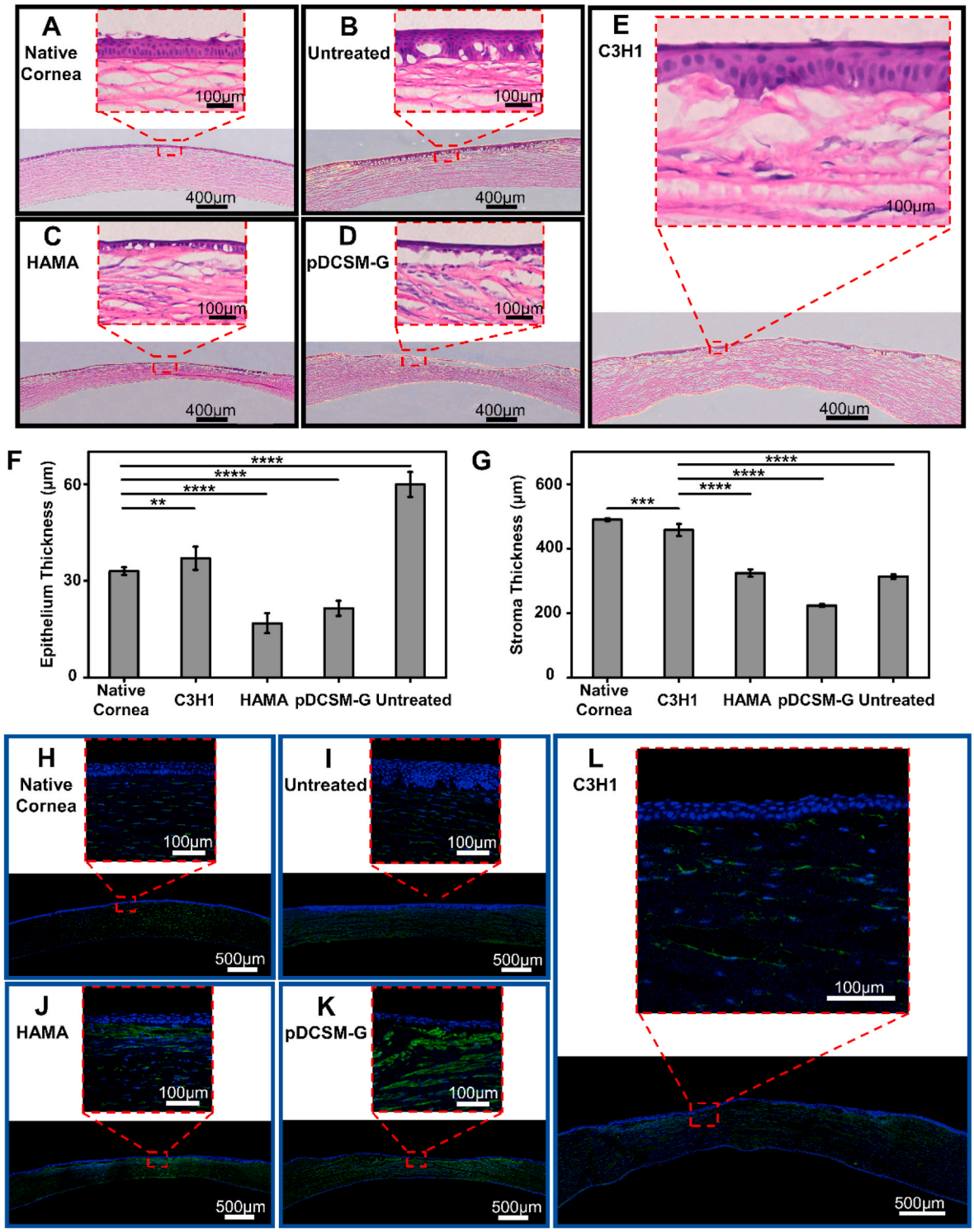

Fig. 7. Histological analysis of the hydrogel treated rabbit corneas eight weeks post-operation. Representative H&E images of (A) native corneas without defect, (B) corneas with untreated defect, and the defected corneas filled with (C) 1% HAMA hydrogel, (D) 3% pDCSM-G, and (E) C3H1 hydrogel. Quantification of (F) epithelium thickness and (G) stroma thickness according to the results from H&E staining. Representative images of immunofluorescence stained (H) native corneas without defect, (I) corneas with untreated defect, and the defected corneas filled with (J) 1% HAMA hydrogel, (K) 3% pDCSM-G, and (L) C3H1 hydrogel, using biomarkers α-SMA (green) and DAPI (blue). (*P < 0.01, ****P < 0.0001).

constantly high transparency, minimal host tissue rejection/inflammation, and promotes cornea-fitting regeneration. Therefore, a dual-crosslinked hybrid hydrogel was prepared and examined in this study, due to the formation of chemically crosslinked double-network that usually leads to highly enhanced mechanical properties and stability.

4.1. Materials selection

Cornea-derived extracellular matrix hydrogel usually forms spontaneously at 37 °C through physical crosslinking. It exhibits much weaker mechanical strength and poor transparency (Fig. 2A, II), especially when compared to the native cornea which has a well-organized extracellular

matrix structure [44,57]. Hence, a suitable dECM hydrogel crosslinker is highly desired. 1-Ethyl-3-(3-dimethylamino-propyl) carbodiimide (EDC)/NHS is a commonly used crosslinker for collagen hydrogels, which was employed in corneal substitute fabricated from recombinant human collagen type III (RHCIII) [7]. However, the EDC coupling reaction is too fast to be controlled, and only can be performed at low temperatures. The extremely short operating window brings big troubles to the process of wound filling and corneal curvature reconstruction during operation. CMC is a viable alternative to EDC. Its larger pendent groups can effectively slow down the crosslinking reaction and provide sufficient operating window at room temperature [45]. More importantly, CMC/NHS crosslinking system has been proven not to participate in the final crosslinked products and toxic-free on the living organization [45,46,56]. Therefore, we chose CMC/NHS as the chemical crosslinker to form the first pDCSM-G polymer network.

HA distributes throughout the body, from the vitreous of the eye to the synovial fluid. Natural HA again has very weak mechanical properties and rapid degradation behavior. One effective way to solve this problem is to chemically modify HA, so that the polysaccharide can be crosslinked [58]. We herein functionalized HA with methacrylic anhydride to produce photocrosslinkable HAMA in the presence of the photoinitiator LAP, This photo-reaction is efficient and easy to implement, which was previously used to seal corneal lacerations [48]. Considering the high biocompatibility and outstanding suitability in ophthalmology, HAMA was employed to crosslink around the pDCSM-G network, to achieve a more robust double-network hydrogel. HAMA plays the dominant role in maintaining the shape and structural stability of the hydrogel [35,59], while pDCSM-G contributes mainly to the cell adhesion and regeneration capacity. The mixture of the hybrid pre-gel solution can be easily applied to the corneal defects. After obtaining a suitable corneal curvature, the viscous pre-gel solution was expose to UV light for only 1 min, which enabled sealing of any irregular-shaped defects, and intimately adhered to the stroma bed (Fig. 1A).

4.2. Physical properties of the dual-crosslinked hydrogel

Our experiments first demonstrated that the dual-crosslinked pDCSM/HAMA hydrogels can provide several special assets to corneal defect treatments, such as high visible light transmittance, limited swelling, and slow degradation properties. The high transparency of the hybrid hydrogels might be attributed to the denser and more orderly distributed polymer network induced by chemical crosslinking [60]. Besides that excellent transparency is key in ophthalmological applications, the lower swelling ratio ensures that the hydrogel can be perfectly docked with the recipient cornea, to prevent shedding from the stromal bed due to excessive swelling. Our results further revealed that increasing the composition of pDCSM in the hybrid hydrogel reduced the swelling ratio accordingly, which is attributed to the higher crosslinking density. Meanwhile, the much lower degradation rate may guarantee that the hydrogel can preserve in the corneal defect to promote corneal tissue regeneration in months. Once the cornea is damaged, the expression of collagenase and metalloproteinase in the corneal cells increases spontaneous to remodel the matrix [47], which can also accelerate the degradation of the protein-based hydrogels. We found that the integration of HAMA can effectively decrease the degradation rate of the hybrid hydrogel with the presence of collagenase type I, which can be slightly manipulated by tuning the pDCSM/HAMA compositions.

Furthermore, the construction of both chemically crosslinked pDCSM-G and HAMA double-network significantly elevated the mechanical properties of the hydrogel, including storage modulus, compressive modulus, shear strength, and bursting pressure, which allows strong resistance to various external or internal forces (Fig. 3). Especially, our dual crosslinked hydrogels achieved much higher shear strength than the commercial surgical sealants, such as fibrin glue (12 ± 6 kPa) [61] and CoSEAL (19 ± 17 kPa) [25]. It was also noticed that the abovementioned mechanical properties were enhanced with increasing the composition of pDCSM content into the same concentration of HAMA (1%, w/v), mostly due to the higher crosslinking density within the hydrogel networks. The formation of stable amide bond not only occurs between the amino and carboxyl groups of pDCSM components, but also reacts with the adjacent tissue in the presence of CMC/NHS, making the hydrogel firmly bind to the tissue, which can resist more than 10 times of the normal IOP in healthy human eyes. The strong adhesion of the hydrogel to the adjacent corneal tissue enabled sutureless operation on the damaged stroma, which may effectively reduce the suture-related postoperative complications, especially for the repair of focal corneal defects.

4.3. Biological properties of the dual-crosslinked hydrogel

An ideal hydrogel for corneal defect repair not only has good biocompatibility, but also supports adhesion and growth of corneal cells and help maintaining the normal cell phenotype. Previous studies and our results demonstrated that HAMA exhibits poor cell adhesion to corneal cells [34,35] owing to the minimal protein adsorption [58] (Fig. 4A and D). Consistent with the results of *in vitro* cell study, the HAMA hydrogel exhibited an extremely negative effect on corneal re-epithelialization in *vivo* (Fig. 6A). The observation of partial epithelialization after 6 weeks was possibly due to the degradation of the HAMA hydrogel, resulting in epithelial cells migration on the exposed host corneal stroma. The pDCSM-G components effectively facilitated the epithelial cells adhesion, achieving fast and complete re-epithelialization on the C3H1 hydrogel treated corneas. Moreover, compared to the HAMA hydrogel alone, the dual-crosslinked C3H1 hydrogel was proven to support the adhesion, viability, and proliferation of the corneal stromal cells (Fig. 4D∼F).

When encountering corneal infections, injuries, or surgeries, quiescent corneal keratocytes are activated to transform into myofibroblasts, which can secrete contractile and irregular extracellular matrix, resulting in formation of corneal scars that severely affects the vision outcomes even after treatments [47]. Therefore, maintaining the cellular phenotype of keratocytes is essential to corneal stroma defect repair. The upregulated expression levels of keratocan and lumican implicated that the C3H1 hydrogel contributed to the maintenance of the normal corneal cell phenotype, rather than transformation into myofibroblasts, which was evident by the downregulation of myofibroblast-related gene expression. Furthermore, the critical corneal proteoglycan lumican not only participates in regulating the growth of collagen fibrils, controlling the structure and function of the cornea, but also plays an important role in maintaining corneal transparency [62]. In a previous report, the lumican-deficient ($Lum^{-/-}$) mice had cloudy corneas while being 40% thinner than those of the wild type mice [63]. The corneal wound healing of $Lum^{-/-}$ mice was also delayed [64]. Therefore, significant upregulation of lumican expression in corneal stromal cells cultured on the C3H1 hydrogel may help maintaining corneal transparency and promoting corneal regeneration. Our *in vivo* study further confirmed that significant scarring occurred at the defected sites of both HAMA and pDCSM-G treated eyes, which was evident by AS-OCT imaging, Masson trichrome staining, and immunostaining on α-SMA expression (Fig. 6B, Fig. S11, and Fig. 7J and K). This result was consistent with the qRT-PCR analysis on the corneal stromal cells *in vitro*, indicating that the C3H1 hydrogel led to a scarless wound healing, in other words, contributed actively to corneal stroma reconstruction. Consequentially, the slit lamp observations showed that the C3H1 hydrogel-filled corneas exhibited excellent transparency, while the HAMA- and pDCSM-G-filled corneas remained opaque (Fig. 6B). Corneal endothelial cells, which play an important role in maintaining corneal transparency and barrier function, are usually sensitive to external stimulation. The results using *in vivo* confocal microscopy showed that the endothelial layer remained intact in C3H1 hydrogel filled corneas eight weeks post-operation, indicating that no excessive damage was induced by the transient UV

irradiation.

Previous reports showed that collagen, GAG, and other active factors in the corneal dECM can effectively promote re-epithelialization and stroma regeneration. For example, Zhou et al. used the pDCSM-G to repair epithelial defect in rats without ablating the corneal stroma [44]. Wang et al. filled the CMC/NHS crosslinked pDCSM-G into a rabbit corneal defect model, demonstrated its biological function in promoting epithelial recovery and matrix regeneration [56]. However, our *in vivo* study implied that the pDCSM-G alone was not sufficient for long-term repair of the defected corneal stroma. On the pDCSM-G filled eye, the reformed epithelium was too thin, and corneal scars also developed 8 weeks post-surgery (Fig. 7D and K). These side effects might be alleviated by using milder decellularization and/or digestion protocols, so that more active ECM components can be preserved. Whereas the pDCSM-G still degraded fast even after CMC/NHS crosslinking. In the meantime, we showed that the pDSCM-G containing dual-crosslinked hydrogel provides a pro-regenerative microenvironment for corneal stromal cells and support cell growth, reduce corneal scarring, promote the secretion of decellularized matrix, and accelerate corneal defect repair (Fig. 7E and L).

Taken together, we herein demonstrated that the dual-crosslinked hydrogel nicely combined the advantages of both pDCSM-G and HAMA hydrogel. The bioactive components of pDCSM-G facilitated corneal cell adhesion, epithelial recovery, stromal regeneration, and maintained inhibitory to corneal fibrosis/scarring. While the introduction of HAMA strongly supported the long-term retention of the hybrid hydrogel. Throughout eight weeks of observation, the experimental eyes filled with C3H1 hydrogel remained transparent, the thicknesses of the epithelial layer and stroma were comparable to those of the native corneas, respectively.

5. Conclusions

In this study, we developed a chemically dual-crosslinked hydrogel consisting of pDCSM-G and HAMA, which can be conveniently filled into corneal defects for sutureless repair, avoiding invasive surgery and complications associated with donor cornea transplantation or preformed hydrogel implantation. Its pDCSM-G components rendered superior biological properties, while the composition of HAMA improved the mechanical strength and stability. The hydrogel exhibited good physical properties for ophthalmological applications, including high transparency, minimal swelling, slow degradation, and enhanced mechanical strength. Furthermore, owing to the formation of interpenetrating network and stable amide bond against the adjacent tissue, this hybrid hydrogel showed excellent sealing performance to achieve sutureless. *In vitro* cell studies indicated that the hydrogel has good cytocompatibility, which effectively supported the adhesion, viability, and proliferation of corneal cells, and maintained keratocyte phenotype of the primary stromal cells. In the eight-week *in vivo* assessments, the experimental eyes filled with dual-crosslinked hydrogel remained transparent, adhered intimately to the stroma bed with a long-term retention, which showed superior performance in reducing corneal scarring, accelerating corneal epithelial and stromal wound healing. Serving as a filling biomaterial and bioactive sealant, the dual-crosslinked hybrid hydrogel is of great promise for long-term repair of corneal defects in future biomedical applications.

Ethics approval and consent to participate

No human participants, human data or human tissue was involved in this manuscript reporting study.

All animal studies were performed in compliance with the Association for Research in Vision and Ophthalmology (ARVO) Statement for the Use of Animals in Ophthalmology and Vision Research. All experiments were approved by the Animal Care Committees of Zhongshan Ophthalmic Center, Sun Yat-sen University.

CRediT authorship contribution statement

Xuanren Shen: Methodology, Validation, Formal analysis, Investigation, Visualization, Writing – original draft. **Saiqun Li:** Conceptualization, Methodology, Investigation, Formal analysis, Writing – review & editing. **Xuan Zhao:** Validation, Investigation, Visualization. **Jiandong Han:** Investigation. **Jiaxin Chen:** Investigation, Visualization. **Zilong Rao:** Investigation. **Kexin Zhang:** Investigation. **Daping Quan:** Conceptualization, Methodology. **Jin Yuan:** Supervision, Project administration, Funding acquisition. **Ying Bai:** Conceptualization, Methodology, Writing – review & editing, Supervision, Project administration, Funding acquisition.

Declaration of competing interest

There are no conflicts of interest in this work.

Acknowledgements

This research was supported by National Key Research and Development Program of China (2018YFC1106001), National Natural Science Foundation of China (51903255, 32171353), Science and Technology Projects in Guangzhou (202002020078), and the Open Research Funds of the State Key Laboratory of Ophthalmology. The authors thank Prof. Zhichong Wang for providing the artificial anterior chamber.

Appendix A. Supplementary data

Supplementary data to this article can be found online at https://doi.org/10.1016/j.bioactmat.2022.06.006.

References

[1] R.N. Palchesko, S.D. Carrasquilla, A.W. Feinberg, Natural biomaterials for corneal tissue engineering, repair, and regeneration, Adv Healthc Mater 7 (16) (2018), e1701434.
[2] A.V. Ljubimov, M. Saghizadeh, Progress in corneal wound healing, Prog. Retin. Eye Res. 49 (2015) 17–45.
[3] P. Gain, R. Jullienne, Z. He, M. Aldossary, S. Acquart, F. Cognasse, G. Thuret, Global survey of corneal transplantation and eye banking, JAMA Ophthalmol 134 (2) (2016) 167–173.
[4] B. Kharod-Dholakia, J.B. Randleman, J.G. Bromley, R.D. Stulting, Prevention and treatment of corneal graft rejection: current practice patterns of the cornea society (2011), Cornea 34 (2015) 609–614.
[5] K. Nishida, M. Yamato, Y. Hayashida, H. Watanabe, T. Okano, Y. Tano, Corneal reconstruction with tissue-engineered cell sheets composed of autologous oral mucosal epithelium, N. Engl. J. Med. 351 (2004) 1187–1196.
[6] S. Matthyssen, B. Van den Bogerd, S.N. Dhubhghaill, C. Koppen, N. Zakaria, Corneal regeneration: a review of stromal replacements, Acta Biomater. 69 (2018) 31–41.
[7] P. Fagerholm, N.S. Lagali, J.A. Ong, K. Merrett, W.B. Jackson, J.W. Polarek, E. J. Suuronen, Y. Liu, I. Brunette, M. Griffith, Stable corneal regeneration four years after implantation of a cell-free recombinant human collagen scaffold, Biomaterials 35 (8) (2014) 2420–2427.
[8] M. Ahearne, J. Fernández-Pérez, S. Masterton, P.W. Madden, P. Bhattacharjee, Designing scaffolds for corneal regeneration, Adv. Funct. Mater. 30 (44) (2020), 1908996.
[9] B. Kong, Y. Chen, R. Liu, X. Liu, C. Liu, Z. Shao, L. Xiong, X. Liu, W. Sun, S. Mi, Fiber reinforced GelMA hydrogel to induce the regeneration of corneal stroma, Nat. Commun. 11 (1) (2020) 1435.
[10] M. Rafat, M. Xeroudaki, M. Koulikovska, P. Sherrell, F. Groth, P. Fagerholm, N. Lagali, Composite core-and-skirt collagen hydrogels with differential degradation for corneal therapeutic applications, Biomaterials 83 (2016) 142–155.
[11] W. Liu, C. Deng, C.R. McLaughlin, P. Fagerholm, N.S. Lagali, B. Heyne, J. C. Scaiano, M.A. Watsky, Y. Kato, R. Munger, N. Shinozaki, F. Li, M. Griffith, Collagen-phosphorylcholine interpenetrating network hydrogels as corneal substitutes, Biomaterials 30 (8) (2009) 1551–1559.
[12] B. Kong, L. Sun, R. Liu, Y. Chen, Y. Shang, H. Tan, Y. Zhao, L. Sun, Recombinant human collagen hydrogels with hierarchically ordered microstructures for corneal stroma regeneration, Chem. Eng. J. 428 (2022), 131012.
[13] Z. Mutlu, S. Shams Es-Haghi, M. Cakmak, Recent trends in advanced contact lenses, Adv Healthc Mater 8 (10) (2019), e1801390.
[14] S. Amjadi, S. Rajak, H. Solanki, D. Selva, Complications related to sutures following penetrating and deep anterior lamellar keratoplasty, Clin. Exp. Ophthalmol. 44 (2) (2015) 142–143.

[15] L. Li, C. Lu, L. Wang, M. Chen, J. White, X. Hao, K.M. McLean, H. Chen, T. C. Hughes, Gelatin-based photocurable hydrogels for corneal wound repair, ACS Appl. Mater. Interfaces 10 (16) (2018) 13283–13292.

[16] C.D. McTiernan, F.C. Simpson, M. Haagdorens, C.D. McTiernan, F.C. Simpson, M. Haagdorens, M.K. Ljunggren, B.D. Allan, M. Griffith, LiQD Cornea: pro-regeneration collagen mimetics as patches and alternatives to corneal transplantation, Sci. Adv. 6 (2020), eaba2187.

[17] G. Trujillo-de Santiago, R. Sharifi, K. Yue, E.S. Sani, S.S. Kashaf, M.M. Alvarez, J. Leijten, A. Khademhosseini, R. Dana, N. Annabi, Ocular adhesives: design, chemistry, crosslinking mechanisms, and applications, Biomaterials 197 (2019) 345–367.

[18] C. Jumelle, A. Yung, E.S. Sani, Y. Taketani, F. Gantin, L. Bourel, S. Wang, E. Yuksel, S. Seneca, N. Annabi, R. Dana, Development and characterization of a hydrogel-based adhesive patch for sealing open-globe injuries, Acta Biomater. 137 (2022) 53–63.

[19] J.L. Alió, E. Mulet, H.F. Sakla, F. Gobbi, Efficacy of synthetic and biological bioadhesives in scleral tunnel phacoemulsification in eyes with high myopia, J. Cataract Refract. Surg. 24 (7) (1998) 983–988.

[20] A.B. Leahey, J.D. Gottsch, W.J. Stark, Clinical experience with N-butyl cyanoacryiate (nexacryl) tissue adhesive, Ophthalmology 100 (2) (1993) 173–180.

[21] M. Mehdizadeh, J. Yang, Design strategies and applications of tissue bioadhesives, Macromol. Biosci. 13 (3) (2013) 271–288.

[22] J. Tan, L.J.R. Foster, S.L. Watson, Corneal sealants in clinical use: a systematic review, Curr. Eye Res. 45 (9) (2020) 1025–1030.

[23] H.J. Lee, G.M. Fernandes-Cunha, K.S. Na, S.M. Hull, D. Myung, Bio-Orthogonally crosslinked, in situ forming corneal stromal tissue substitute, Adv Healthc Mater 7 (19) (2018), e1800560.

[24] G. Yazdanpanah, X. Shen, T. Nguyen, K.N. Anwar, O. Jeon, Y. Jiang, M. Pachenari, Y. Pan, T. Shokuhfar, M.I. Rosenblatt, E. Alsberg, A.R. Djalilian, A light-curable and tunable extracellular matrix hydrogel for in situ suture-free corneal repair, Adv. Funct. Mater. (2022), 2113383.

[25] E.S. Sani, A. Kheirkhah, D. Rana, Z. Sun, W. Foulsham, A. Sheikhi, A. Khademhosseini, R. Dana, N. Annabi, Sutureless repair of corneal injuries using naturally derived bioadhesive hydrogels, Sci. Adv. 5 (2019), eaav1281.

[26] Y. Zhang, C. Li, Q. Zhu, R. Liang, C. Xie, S. Zhang, Y. Hong, H. Ouyang, A long-term retaining molecular coating for corneal regeneration, Bioact. Mater. 6 (12) (2021) 4447–4454.

[27] Y. Liu, L. Ren, Y. Wang, Crosslinked collagen-gelatin-hyaluronic acid biomimetic film for cornea tissue engineering applications, Mater Sci Eng C Mater Biol Appl 33 (1) (2013) 196–201.

[28] N. Mitrousis, S. Hacibekiroglu, M.T. Ho, Y. Sauve, A. Nagy, D. van der Kooy, M. S. Shoichet, Hydrogel-mediated co-transplantation of retinal pigmented epithelium and photoreceptors restores vision in an animal model of advanced retinal degeneration, Biomaterials 257 (2020), 120233.

[29] E. Eljarrat-Binstock, J. Pe'er, A.J. Domb, New techniques for drug delivery to the posterior eye segment, Pharm. Res. (N. Y.) 27 (4) (2010) 530–543.

[30] A.E.G. Baker, H. Cui, B.G. Ballios, S. Ing, P. Yan, J. Wolfer, T. Wright, M. Dang, N. Y. Gan, M.J. Cooke, A. Ortin-Martinez, V.A. Wallace, D. van der Kooy, R. Devenyi, M.S. Shoichet, Stable oxime-crosslinked hyaluronan-based hydrogel as a biomimetic vitreous substitute, Biomaterials 271 (2021), 120750.

[31] F. Chen, P. Le, G.M. Fernandes-Cunha, S.C. Heilshorn, D. Myung, Bio-orthogonally crosslinked hyaluronate-collagen hydrogel for suture-free corneal defect repair, Biomaterials 255 (2020), 120176.

[32] G.M. Fernandes-Cunha, S.H. Jeong, C.M. Logan, P. Le, D. Mundy, F. Chen, K. M. Chen, M. Kim, G.H. Lee, K.S. Na, S.K. Hahn, D. Myung, Supramolecular host-guest hyaluronic acid hydrogels enhance corneal wound healing through dynamic spatiotemporal effects, Ocul. Surf. 23 (2022) 148–161.

[33] L. Koivusalo, M. Kauppila, S. Samanta, V.S. Parihar, T. Ilmarinen, S. Miettinen, O. P. Oommen, H. Skottman, Tissue adhesive hyaluronic acid hydrogels for sutureless stem cell delivery and regeneration of corneal epithelium and stroma, Biomaterials 225 (2019), 119516.

[34] F. Chen, P. Le, K. Lai, G.M. Fernandes-Cunha, D. Myung, Simultaneous interpenetrating polymer network of collagen and hyaluronic acid as an in situ-forming corneal defect filler, Chem. Mater. 32 (12) (2020) 5208–5216.

[35] H.J. Lee, G.M. Fernandes-Cunha, D. Myung, In situ-forming hyaluronic acid hydrogel through visible light-induced thiol-ene reaction, React. Funct. Polym. 131 (2018) 29–35.

[36] X. Zhang, X. Chen, H. Hong, R. Hu, J. Liu, C. Liu, Decellularized extracellular matrix scaffolds: recent trends and emerging strategies in tissue engineering, Bioact. Mater. 10 (2022) 15–31.

[37] Z. Rao, T. Lin, S. Qiu, J. Zhou, S. Liu, S. Chen, T. Wang, X. Liu, Q. Zhu, Y. Bai, D. Quan, Decellularized nerve matrix hydrogel scaffolds with longitudinally oriented and size-tunable microchannels for peripheral nerve regeneration, Mater Sci Eng C Mater Biol Appl 120 (2021), 111791.

[38] S. Liu, Z. Rao, J. Zou, S. Chen, Q. Zhu, X. Liu, Y. Bai, Y. Liu, D. Quan, Properties regulation and biological applications of decellularized peripheral nerve matrix hydrogel, ACS Appl. Bio Mater. 4 (8) (2021) 6473–6487.

[39] Y. Xu, J. Zhou, C. Liu, S. Zhang, F. Gao, W. Guo, X. Sun, C. Zhang, H. Li, Z. Rao, S. Qiu, Q. Zhu, X. Liu, X. Guo, Z. Shao, Y. Bai, X. Zhang, D. Quan, Understanding the role of tissue-specific decellularized spinal cord matrix hydrogel for neural stem/progenitor cell microenvironment reconstruction and spinal cord injury, Biomaterials 268 (2021), 120596.

[40] M.C. Zhang, X. Liu, Y. Jin, D.L. Jiang, X.S. Wei, H.T. Xie, Lamellar keratoplasty treatment of fungal corneal ulcers with acellular porcine corneal stroma, Am. J. Transplant. 15 (4) (2015) 1068–1075.

[41] J. Fernandez-Perez, M. Ahearne, Decellularization and recellularization of cornea: progress towards a donor alternative, Methods 171 (2020) 86–96.

[42] H. Yin, Q. Lu, X. Wang, S. Majumdar, A.S. Jun, W.J. Stark, M.P. Grant, J. H. Elisseeff, Tissue-derived microparticles reduce inflammation and fibrosis in cornea wounds, Acta Biomater. 85 (2019) 192–202.

[43] D. Bejleri, M.E. Davis, Decellularized extracellular matrix materials for cardiac repair and regeneration, Adv Healthc Mater 8 (5) (2019), e1801217.

[44] Q. Zhou, V.H. Guaiquil, M. Wong, A. Escobar, E. Ivakhnitskaia, G. Yazdanpanah, H. Jing, M. Sun, J. Sarkar, Y. Luo, M.I. Rosenblatt, Hydrogels derived from acellular porcine corneal stroma enhance corneal wound healing, Acta Biomater. 134 (2021) 177–189.

[45] J.I. Ahn, L. Kuffova, K. Merrett, D. Mitra, J.V. Forrester, F. Li, M. Griffith, Crosslinked collagen hydrogels as corneal implants: effects of sterically bulky vs. non-bulky carbodiimides as crosslinkers, Acta Biomater. 9 (8) (2013) 7796–7805.

[46] C. Molzer, S.P. Shankar, V. Masalski, M. Griffith, L. Kuffova, J.V. Forrester, TGF-beta1-activated type 2 dendritic cells promote wound healing and induce fibroblasts to express tenascin c following corneal full-thickness hydrogel transplantation, J Tissue Eng Regen Med 13 (9) (2019) 1507–1517.

[47] J.A. West-Mays, D.J. Dwivedi, The keratocyte: corneal stromal cell with variable repair phenotypes, Int. J. Biochem. Cell Biol. 38 (10) (2006) 1625–1631.

[48] D. Miki, K. Dastgheib, T. Kim, A. Pfister-Serres, K.A. Smeds, M. Inoue, D. L. Hatchell, M.W. Grinstaff, A photopolymerized sealant for corneal lacerations, Cornea 21 (4) (2002) 393–399.

[49] C. Zhao, Z. Wu, H. Chu, T. Wang, S. Qiu, J. Zhou, Q. Zhu, X. Liu, D. Quan, Y. Bai, Thiol-rich multifunctional macromolecular crosslinker for gelatin-norbornene-based bioprinting, Biomacromolecules 22 (6) (2021) 2729–2739.

[50] X. Wang, Y. Yu, C. Yang, C. Shao, K. Shi, L. Shang, F. Ye, Y. Zhao, Microfluidic 3D printing responsive scaffolds with biomimetic enrichment channels for bone regeneration, Adv. Funct. Mater. 31 (40) (2021), 2105190.

[51] L. Zilic, S.P. Wilshaw, J.W. Haycock, Decellularisation and histological characterisation of porcine peripheral nerves, Biotechnol. Bioeng. 113 (9) (2016) 2041–2053.

[52] S. Xiong, H. Gao, L. Qin, Y.G. Jia, L. Ren, Engineering topography: effects on corneal cell behavior and integration into corneal tissue engineering, Bioact. Mater. 4 (2019) 293–302.

[53] S.G. Scott, A.S. Jun, S. Chakravarti, Sphere formation from corneal keratocytes and phenotype specific markers, Exp. Eye Res. 93 (6) (2011) 898–905.

[54] G. Yazdanpanah, R. Shah, R.S.S. Raghurama, K.N. Anwar, X. Shen, S. An, M. Omidi, M.I. Rosenblatt, T. Shokuhfar, A.R. Djalilian, In-situ porcine corneal matrix hydrogel as ocular surface bandage, Ocul. Surf. 21 (2021) 27–36.

[55] S. Chameettachal, D. Prasad, Y. Parekh, S. Basu, V. Singh, K.K. Bokara, F. Pati, Prevention of corneal myofibroblastic differentiation in vitro using a biomimetic ECM hydrogel for corneal tissue regeneration, ACS Appl. Bio Mater. 4 (1) (2021) 533–544.

[56] F. Wang, W. Shi, H. Li, H. Wang, D. Sun, L. Zhao, L. Yang, T. Liu, Q. Zhou, L. Xie, Decellularized porcine cornea-derived hydrogels for the regeneration of epithelium and stroma in focal corneal defects, Ocul. Surf. 18 (4) (2020) 748–760.

[57] K.M. Meek, Corneal collagen-its role in maintaining corneal shape and transparency, Biophys Rev 1 (2) (2009) 83–93.

[58] J.A. Burdick, G.D. Prestwich, Hyaluronic acid hydrogels for biomedical applications, Adv. Mater. 23 (12) (2011) H41–H56.

[59] M.D. Brigham, A. Bick, E. Lo, A. Bendali, J.A. Burdick, A. Khademhosseini, Mechanically robust and bioadhesive collagen and photocrosslinkable hyaluronic acid semi-interpenetrating networks, Tissue Eng. 15 (2009) 1645–1653.

[60] X. Duan, H. Sheardown, Dendrimer crosslinked collagen as a corneal tissue engineering scaffold: mechanical properties and corneal epithelial cell interactions, Biomaterials 27 (26) (2006) 4608–4617.

[61] X. Zhao, S. Li, X. Du, W. Li, Q. Wang, D. He, J. Yuan, Natural polymer-derived photocurable bioadhesive hydrogels for sutureless keratoplasty, Bioact. Mater. 8 (2022) 196–209.

[62] Andrew J. Quantock, K.M. Meek, S. Chakravarti, An X-ray diffraction investigation of corneal structure in lumican-deficient mice, Investig. Ophthalmol. Vis. Sci. 42 (2001) 1750–1756.

[63] H. Shao, R. Chaerkady, S. Chen, S.M. Pinto, R. Sharma, B. Delanghe, D.E. Birk, A. Pandey, S. Chakravarti, Proteome profiling of wild type and lumican-deficient mouse corneas, J. Proteonomics 74 (10) (2011) 1895–1905.

[64] N. Vij, L. Roberts, S. Joyce, S. Chakravarti, Lumican suppresses cell proliferation and aids Fas-Fas ligand mediated apoptosis: implications in the cornea, Exp. Eye Res. 78 (5) (2004) 957–971.